A LOW-COMPLEXITY 3D SPATIO-TEMPORAL FIR FILTER FOR ENHANCING LINEAR TRAJECTORY SIGNALS

Chamira U. S. Edussooriya[⋆], *Len T. Bruton*[†] *and Panajotis Agathoklis*[⋆]

[⋆]Department of Electrical and Computer Engineering, University of Victoria, Victoria, BC, Canada
[†]Department of Electrical and Computer Engineering, University of Calgary, Calgary, AB, Canada

ABSTRACT

A low-complexity 3D FIR filter is proposed for selectively enhancing severely corrupted linear trajectory spatio-temporal signals. The proposed 3D FIR filter is separable and consists of a 3D spatio-temporal wide-angle FIR cone filter between two 2D spatial variable-shift filters. Low complexity of the 3D spatio-temporal wide-angle FIR cone filter is achieved by exploiting the spatial-symmetry of the passband and by employing maximal decimation in the temporal dimension. Compared to existing techniques, the proposed 3D FIR filter provides significant reduction of the computational complexity for similar SINR improvement.

Index Terms— 3D FIR filtering, linear trajectory filter, velocity filter, video enhancement, cone-stop filtering.

1. INTRODUCTION

There are many applications including traffic analysis, radar tracking and computer vision, where enhancement of objects moving with *approximately constant* 2D spatial velocities over local regions are required [1]–[3]. A 3D spatio-temporal signal representing such a moving object, ideally with a constant 2D spatial velocity, is called a linear trajectory (LT) signal. In previously reported methods, 3D FIR and IIR filters having planar-shaped passbands [4]–[6] or wedge-shaped (exterior of a wide-angle cone) passbands [7]–[11] have been employed to process LT signals. In general, these passbands are not symmetric with respect to the temporal frequency axis.

In this paper, a low-complexity 3D FIR filter is proposed to enhance severely corrupted LT signals. In the proposed 3D FIR filter, the 3D input signal is subjected to 2D spatial shifts before selectively filtering with a low-complexity 3D spatio-temporal wide-angle FIR cone filter. The use of 2D spatial shifts, motivated by *the temporal delaying in conventional delay-and-sum beamformers* [12](ch. 6)–[14], has the effect of rotating the region of support of the spectrum of a LT signal to be *symmetric with respect to the temporal frequency axis*. Consequently, the passband of the 3D spatio-temporal FIR cone filter can be approximated by a low-complexity filter bank structure similar to the one proposed in [15]. Numerical simulations indicate that the proposed 3D FIR filter provides significant reduction of the computational complexity compared to existing techniques for similar signal-to-interference-and-noise ratio (SINR) improvement.

The organization of the paper is as follows. A review of LT signals and their spectra is presented in Section 2. In Section 3, the proposed 3D FIR filter is described in detail. Numerical simulation results are presented in Section 4. Finally, conclusion and future work are presented in Section 5.

2. REVIEW OF LT SIGNALS AND THEIR SPECTRA

Let us consider a sampled LT signal having an object moving with a constant 2D spatial velocity $[v_x \ \ v_y]^{\mathrm{T}}$. Under the *constant intensity assumption*, the 3D intensity of the object, $I(n_x, n_y, n_t)$, $(n_x, n_y, n_t) \in \mathbb{Z}^3$, may be written as

$$I(n_x, n_y, n_t) = I_R(n_x - \Delta x(n_t), n_y - \Delta y(n_t), n_{t0}), \quad (1)$$

where $I_R(x, y, n_{t0})$ is the 2D intensity of the object at $n_t = n_{t0}$ (considered as the reference frame), and $\Delta x(n_t)$ and $\Delta y(n_t)$ are, respectively, the displacements (in pixels) of the object along the x and y dimensions (with respect to the reference frame) at n_t and are, respectively, given by [16](pp. 40)

$$\Delta x(n_t) = v_x(n_t - n_{t0}) \quad (2a)$$
$$\Delta y(n_t) = v_y(n_t - n_{t0}). \quad (2b)$$

The region of support of the spectrum of such a LT signal is a *plane* going through the origin inside the principal Nyquist cube $(\omega_x, \omega_y, \omega_t) \in \mathbb{R}^3$, $-\pi \leq \omega_x, \omega_y, \omega_t \leq \pi$ [4], [16](pp. 41). The orientation of the plane is determined by the 2D spatial velocity, and the vector normal to the plane is given by $[v_x \ \ v_y \ \ 1]^{\mathrm{T}}$ [16](pp. 41).

3. PROPOSED LOW-COMPLEXITY 3D FIR FILTER

The low-complexity 3D FIR filter that can be employed to selectively enhance LT signals is presented in this section.

The authors gratefully acknowledge the financial support of the Natural Sciences and Engineering Research Council (NSERC) of Canada.

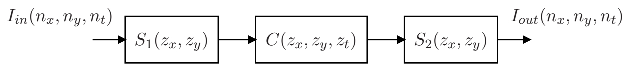

Fig. 1. Proposed low-complexity 3D FIR filter.

The proposed 3D FIR filter, illustrated in Fig. 1, consists of a 3D spatio-temporal wide-angle FIR cone filter, $C(z_x, z_y, z_t)$, $(z_x, z_y, z_t) \in \mathbb{C}^3$, between two 2D spatial variable-shift filters, $S_1(z_x, z_y)$ and $S_2(z_x, z_y)$, $(z_x, z_y) \in \mathbb{C}^2$. To describe the operation of the proposed filter, let us consider a 3D input signal $I_{in}(n_x, n_y, n_t)$ consisting of a LT signal of interest having the 3D intensity $I(n_x, n_y, n_t)$ and moving with $[v_x \;\; v_y]^{\mathrm{T}}$ and interfering signals having 2D spatial velocities other than $[v_x \;\; v_y]^{\mathrm{T}}$. The first 2D spatial variable-shift filter spatially shifts $I_{in}(n_x, n_y, n_t)$ by $[-\Delta x(n_t) \;\; -\Delta y(n_t)]^{\mathrm{T}}$ so that $I(n_x, n_y, n_t)$ is *stationary* with respect to the temporal dimension. This is equivalent to rotating the region of support of the spectrum of $I(n_x, n_y, n_t)$ to lie on the $\omega_x\omega_y$ plane. Note that the regions of support of the spectra of interfering signals occupy regions other than the $\omega_x\omega_y$ plane.

In real applications, $\Delta x(n_t)$ and $\Delta y(n_t)$ are *approximations* of the exact 2D spatial shifts. As a result, after the 2D spatial shifts $[-\Delta x(n_t) \;\; -\Delta y(n_t)]^{\mathrm{T}}$, the region of support of the spectrum of $I(n_x, n_y, n_t)$ may deviate slightly from the $\omega_x\omega_y$ plane. Consequently, the passband of the 3D filter $C(z_x, z_y, z_t)$ employed to selectively enhance the LT signal of interest should be the *exterior* of a wide-angle cone as shown in Fig. 2. Because the passband of $C(z_x, z_y, z_t)$ is *symmetric with respect to the ω_t axis*, the passband can be approximated using a low-complexity 3D spatio-temporal wide-angle FIR cone filter bank as described in Section 3.2.

The second 2D spatial variable-shift filter $S_2(z_x, z_y)$ is used to reverse the 2D artificial spatial shifts introduced by the first 2D spatial variable-shift filter $S_1(z_x, z_y)$.

3.1. Design and Implementation of 2D Spatial Shifts

The 2D spatial shifts are carried out as two 1D spatial shifts for each temporal frame. For most applications, it is sufficient to estimate both $\Delta x(n_t)$ and $\Delta y(n_t)$ to the accuracy of one pixel, i.e. both $\Delta x(n_t)$ and $\Delta y(n_t)$ are *integer valued*. Consequently, for each temporal frame, the 1D spatial shifts are implemented using *circular shifts* along the x and y dimensions. Note that, this does not need any arithmetic operations, and the additional memory requirement is very low.

3.2. Design and Efficient Implementation of 3D Spatio-Temporal Wide-Angle FIR Cone Filter Bank

Here, the design and efficient implementation of the 3D spatio-temporal wide-angle FIR cone filter bank are presented. For brevity, we henceforth call it the cone filter bank. The proposed cone filter bank is structurally similar to the cone and frustum filter bank structure proposed in [15]. The major difference between the cone filter bank in [15] and the proposed cone filter bank is that the former has a cone-shaped passband whereas the latter has a cone-shaped stopband.

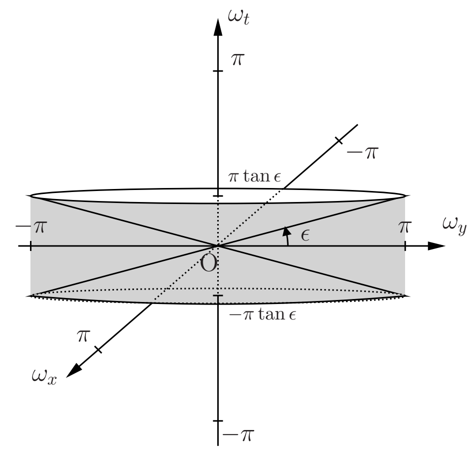

Fig. 2. Ideal passband of $C(z_x, z_y, z_t)$ (in gray colour), which is the exterior of a wide-angle cone, where ϵ is the angle between the $\omega_x\omega_y$ plane and the surface of the wide-angle cone.

The proposed cone filter bank, shown in Fig. 3(a), consists of a 1D temporal modified discrete Fourier transform (DFT) filter bank [17] and 2D spatial FIR filters. These 2D spatial FIR filters include a 2D spatial allpass filter, $2M_h$ 2D spatial circularly symmetric highpass filters and $M - (2M_h + 1)$ 2D spatial allstop filters, where M is the number of bands. For given M and ϵ, M_h is obtained as the integer $k \in \{1, 2, \ldots, M/2 - 1\}$ that minimizes $|(2k+1)/M - \tan\epsilon|$. The passband of the cone filter bank is approximated using the 2D spatial allpass filter and the $2M_h$ 2D spatial circularly symmetric highpass filters as illustrated in Fig. 3(b). The 2D spatial allstop filters are utilized for the stopband.

3.2.1. Design of the 1D Temporal Modified DFT Filter Bank

Both analysis filters $H_k(z_t)$ and synthesis filters $F_k(z_t)$ ($z_t \in \mathbb{C}$ and $k = 0, 1, \ldots, M-1$) of a 1D modified DFT filter bank are obtained by means of uniform complex modulation of a zero-phase FIR lowpass prototype filter $P(z_t)$, having a cut-off frequency π/M [17]. Consequently, the design of the 1D modified DFT filter bank is effectively limited to the design of the prototype filter. For the proposed cone filter bank, the length of the prototype filter is selected as $2M$ since, for this case, the impulse response of the prototype filter, $p(n_t)$, can be given [17], [18], in closed form, as

$$p(n_t) = \frac{-1}{2\sqrt{M}} + \frac{1}{\sqrt{2M}} \cos\left(\frac{\pi}{2M}(2n_t + 2M)\right),$$
$$n_t = -M + 0.5, -M + 1.5, \ldots, M - 0.5. \quad (3)$$

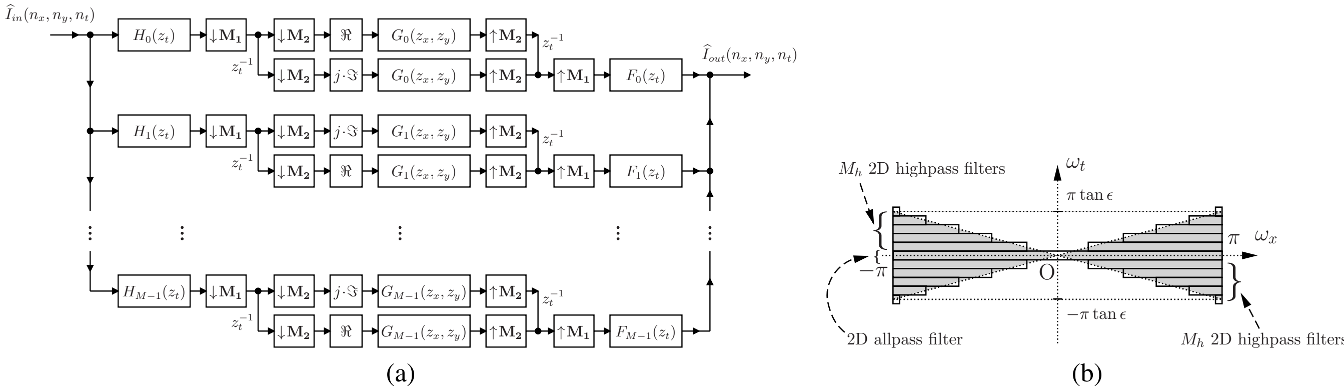

Fig. 3. (a) Proposed 3D spatio-temporal wide-angle FIR cone filter bank, where $\mathbf{M_1} = \mathrm{diag}\,[1\ \ 1\ \ M/2]$ and $\mathbf{M_2} = \mathrm{diag}\,[1\ \ 1\ \ 2]$. (b) Approximation of the passband using a 2D spatial allpass filter and $2M_h$ 2D spatial highpass filters; a planar view on the $\omega_x\omega_t$ plane.

3.2.2. *Design of the 2D Spatial FIR Filters*

The 2D spatial filter corresponding to the 0th band is allpass and its impulse response is given by $g_0(n_x, n_y) = \delta(n_x, n_y)$, where $(n_x, n_y) \in \mathbb{Z}^2$. The 2D spatial filters corresponding to $k = 1, 2, \ldots, M_h$ and $k = M-M_h, M-(M_h+1), \ldots, M-1$ are 2D spatial circularly symmetric highpass filters, and the design is carried out using the windowing technique in conjunction with the 2D circular Hamming window [12](ch. 3), [19](ch. 4). The cutoff frequencies $\omega_{c,k}$ are selected as

$$\omega_{c,k} = \frac{2k\pi}{M}\cot\epsilon, \qquad k = 1, 2, \ldots, M_h, \tag{4}$$

and $\omega_{c,k} = \omega_{c,M-k}$, $k = M-M_h, M-(M_h+1), \ldots, M-1$. The impulse responses of the 2D spatial allstop filters are simply zero, i.e. $g_k(n_x, n_y) = 0$, $k = M_h+1, M_h+2, \ldots, M-(M_h-1)$.

3.2.3. *Near-Perfect Reconstruction and Efficient Implementation of the 3D Spatio-Temporal Wide-Angle FIR Cone Filter Bank*

Following a similar analysis presented in [15], it can be proved that the proposed cone filter bank provides near-perfect reconstruction, and the transfer function is given by

$$C(z_x, z_y, z_t) = \frac{z_t^{-M/2}}{M}\sum_{k=0}^{M-1} H_k(z_t)G_k(z_x, z_y)F_k(z_t). \tag{5}$$

Furthermore, the proposed cone filter bank can be efficiently implemented using the structure proposed for 3D spatio-temporal FIR frustum filters in [15](Fig. 3). Due to the limited space, the efficient implementation is not presented here, and the reader is referred to [15] for more details of the derivation.

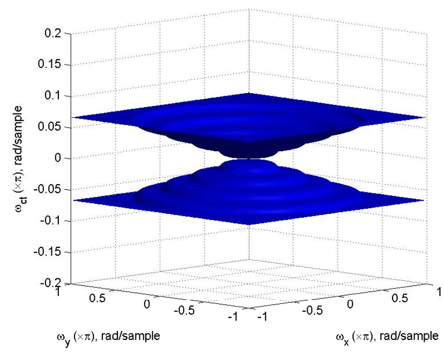

Fig. 4. -3 dB iso-surface of the magnitude response of the 3D spatio-temporal wide-angle FIR cone filter bank.

4. NUMERICAL SIMULATION RESULTS

The performance of the proposed 3D FIR filter in enhancing heavily corrupted approximately LT signals is illustrated in this section. Furthermore, a comparison of the computational complexity of the proposed 3D FIR filter with that of the 3D IIR filter in [7] and the 3D FIR filter in [10] is presented.

For the design of the cone filter bank, M and ϵ are selected as 128 and 4°, respectively. For these values, M_h is obtained as 4, and the order of the 2D spatial circularly symmetric highpass filters is selected as 30×30. The -3 dB iso-surface of the magnitude response of the cone filter bank $C(z_x, z_y, z_t)$ is shown in Fig. 4. It is observed that the magnitude response approximates well the required passband.

4.1. Performance in Enhancing a Heavily Corrupted Approximately LT Signal

In this case, we employ a test video signal, of size $256 \times 256 \times 512$, containing an approximately LT signal of interest

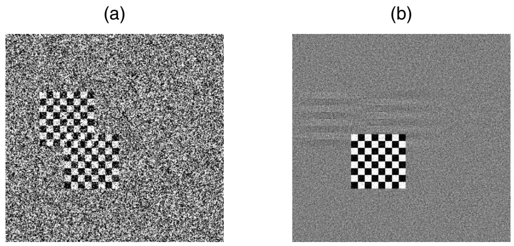

Fig. 5. The 275th frame of (a) 3D input signal (b) 3D output signal

$x_l(n_x, n_y, n_t)$, an interfering signal $x_i(n_x, n_y, n_t)$ and additive white Gaussian noise. Both the LT signal of interest and the interfering signal consist of a highly-detailed black (intensity = -0.5) and white (intensity = $+0.5$) checkerboard $x_c(n_x, n_y, n_t)$ of 64×64 pixels in a gray (intensity = 0) background as in [7], [8]. These two signals are numerically generated as

$$x_l(n_x, n_y, n_t) = x_c(\lceil 5 + 0.1n_t + 0.0005n_t^2 \rceil, \lceil 100 + 0.09n_t - 7\sin(2\pi n_t/800) \rceil, n_t) \quad \text{(6a)}$$

$$x_i(n_x, n_y, n_t) = x_c(\lceil 180 - 0.7n_t + 0.0007n_t^2 \rceil, \lceil 50 + 0.09n_t - 7\sin(2\pi n_t/800) \rceil, n_t), \quad \text{(6b)}$$

where $\lceil \cdot \rceil$ is the ceiling function. The energy of the interfering signal and the noise are selected as the same and 10 times the energy of the LT signal of interest, respectively, to represent a heavily corrupted input signal. The resulting SINR at the input is -10.41 dB. To estimate the SINR at the output, the portion of the 3D output signal corresponding to the temporal steady state, $\{(n_x, n_y, n_t) | 1 \leq n_x, n_y \leq 256, 129 \leq n_t \leq 384\}$, is used. The SINR at the output is 2.84 dB implying a 13.25 dB improvement. The 275th frame of the input and output test video signals are shown in Fig. 5. Note that the LT signal of interest and the interfering signal partially overlap in the input frame, and the LT signal of interest is successfully enhanced by the proposed 3D FIR filter.

4.2. Comparison with Existing Techniques

The number of real multiplications and additions (excluding the trivial multiplications with ± 1 and $\pm j$ and the trivial additions with 0) required to process a sample of a 3D input signal is considered as a measure of the computational complexity. The numerical values for the proposed 3D FIR filter, the 3D IIR filter in [7] and the 3D FIR filter in [10] *having similar passbands and providing similar SINR improvement* are presented in Table 1. Note that the cone filter bank is efficiently implemented using the structure proposed in [15](Fig. 3), which employs maximal decimation in the temporal dimension and the polyphase realization of the 1D modified DFT filter bank. The filters are implemented using direct form structures, and the symmetry of the coefficients are utilized to reduce the number of real multiplications. Furthermore, 2D spatial allpass and allstop filters do not require any arithmetic operations. According to Table 1, the proposed 3D FIR filter provides significant reduction in the computational complexity.

Table 1. Numbers of nontrivial real multiplications and additions required to process a sample of a 3D input signal by different 3D filters.

Filter	Mul.	Add.
Proposed 3D FIR filter	52.84	177.5
3D IIR filter [7]	231	440
3D optimal FIR filter [10]	3375	3374

One disadvantage of the proposed 3D FIR filter compared to the 3D IIR filter in [7] and the 3D FIR filter in [10] is that the proposed 3D FIR filter has a higher temporal group delay due to the high order of the prototype filter employed in the 1D modified DFT filter bank. Furthermore, the proposed 3D FIR filter may provide poor approximation to the ideal passband at frequencies near the origin due to the low number of 2D spatial highpass filters employed in the cone filter bank. This may be partially avoided by employing a 1D *non-uniform* temporal filter bank at the expense of additional computational complexity.

5. CONCLUSION AND FUTURE WORK

A low-complexity 3D FIR filter is proposed for enhancing severely corrupted approximately linear trajectory signals. The proposed 3D FIR filter employs 2D spatial shifts before selectively filtering the 3D input signal with a low-complexity 3D spatio-temporal wide-angle FIR cone filter. The low complexity is achieved by employing maximal decimation in the temporal dimension, by exploiting the symmetry of the passband with respect to the temporal frequency axis and due to the higher percentage of the 2D spatial allpass and allstop filters, which require no arithmetic operations. The effectiveness of the proposed 3D FIR filter in enhancing a heavily corrupted video signal having an approximately linear trajectory signal of interest is demonstrated by using a test video signal. The proposed 3D FIR filter provides significant reduction of the computational complexity compared to existing techniques for similar SINR improvement.

As future work, the proposed 3D FIR filter can be employed to enhance *nonlinear* trajectory signals. In this case, the 3D spatio-temporal wide-angle FIR cone filter is *not* required to be designed adaptively. Only the 2D spatial shifts are required to be implemented adaptively. Consequently, the proposed 3D FIR filter has a great potential to be employed in real-time applications.

6. REFERENCES

[1] L. T. Bruton, N. R. Bartley, and Z. Q. Liu, "On the classification of moving objects in image sequences using 3D adaptive recursive tracking filters and neural networks," in *Proc. 29th Asilomar Conf. Signals, Syst., Comput.*, 1995, vol. 2, pp. 1006–1010.

[2] J.-Y. Chang, C.-C. Cheng, S.-Y. Chien, and L.-G. Chen, "Relative depth layer extraction for monoscopic video by use of multidimensional filter," in *Proc. IEEE Int. Conf. Multimedia and Expo*, 2006, pp. 221–224.

[3] T. Schwerdtfeger, J. Velten, and A. Kummert, "A multidimensional wave digital filter bank for video-based motion analysis," *Multidim. Syst. Signal Processing*, vol. 25, no. 2, pp. 295–311, Apr. 2014.

[4] L. T. Bruton and N. R. Bartley, "Three-dimensional image processing using the concept of network resonance," *IEEE Trans. Circuits Syst.*, vol. CAS-32, no. 7, pp. 664–672, July 1985.

[5] L. T. Bruton and N. Bartley, "The enhancement and tracking of moving objects in digital images using adaptive three-dimensional recursive filters," *IEEE Trans. Circuits Syst.*, vol. CAS-33, no. 6, pp. 604–612, June 1986.

[6] S.-C. Pei, W.-Y. Kuo, and W.-T. Huang, "Tracking moving objects in image sequences using 1-D trajectory filter," *IEEE Signal Process. Lett.*, vol. 13, no. 1, pp. 13–16, Jan. 2006.

[7] B. Kuenzle and L. T. Bruton, "3-D IIR filtering using decimated DFT-polyphase filter bank structures," *IEEE Trans. Circuits Syst. I*, vol. 53, no. 2, pp. 394–408, Feb. 2006.

[8] B. Kuenzle and L. T. Bruton, "A novel low-complexity spatio-temporal ultra wide-angle polyphase cone filter bank applied to sub-pixel motion discrimination," in *Proc. Int. Symp. Circuits Syst.*, 2005, pp. 2397–2400.

[9] S. Schauland, J. Velten, and A. Kummert, "Motion-based object detection for automotive applications using multidimensional wave digital filters," in *Proc. IEEE Veh. Technol. Conf. (VTC Spring)*, 2008, pp. 2700–2704.

[10] K. Kondo and N. Hamada, "Design of optimal filter for detecting linear trajectory signals utilizing object shape and velocity vector," *Electron. and Commun. in Japan, Part I*, vol. 83, no. 2, pp. 42–51, Feb. 2000.

[11] B Anderson and L. T. Bruton, "Non-uniform bandwidth frequency-planar (NUB-FP) filter banks," in *Proc. Int. Symp. Circuits Syst.*, 2002, vol. 1, pp. I–809–I–812.

[12] D. E. Dudgeon and R. M. Mersereau, *Multidimensional Digital Signal Processing*, Prentice-Hall, Englewood Cliffs, NJ, 1984.

[13] B. D. Van Veen and K. M. Buckley, "Beamforming: A versatile approach to spatial filtering," *IEEE ASSP Mag.*, vol. 5, no. 2, pp. 4–24, Apr. 1988.

[14] C. U. S. Edussooriya, L. T. Bruton, M. A. Naeini, and P. Agathoklis, "Using 1-D variable fractional-delay filters to reduce the computational complexity of 3-D broadband multibeam beamformers," *IEEE Trans. Circuits Syst. II*, vol. 61, no. 4, Apr. 2014.

[15] C. U. S. Edussooriya, L. T. Bruton, P. Agathoklis, and T. K. Gunaratne, "Low-complexity maximally-decimated multirate 3D spatio-temporal FIR cone and frustum filters," *IEEE Trans. Circuits Syst. I*, vol. 60, no. 7, pp. 1845–1856, July 2013.

[16] Y. Wang, J. Ostermann, and Y.-Q. Zhang, *Video Processing and Communications*, Prentice-Hall, Upper Saddle River, NJ, 2002.

[17] T. Karp and N. J. Fliege, "Modified DFT filter banks with perfect reconstruction," *IEEE Trans. Circuits Syst. II*, vol. 46, no. 11, pp. 1404–1414, Nov. 1999.

[18] H. S. Malvar, "Extended lapped transforms: properties, applications, and fast algorithms," *IEEE Trans. Signal Process.*, vol. 40, no. 11, pp. 2703–2714, Nov. 1992.

[19] J. S. Lim, *Two-Dimensional Signal and Image Processing*, Prentice-Hall, Upper Saddle River, NJ, 1990.